RESEARCH ARTICLE

Bioprinted Gelatin-Recombinant Type III Collagen Hydrogel Promotes Wound Healing

Jianghong Huang[1,2†], Xiaoling Lei[3†], Zhiwang Huang[1†], Zhibin Rong[4], Haihang Li[5], Yixin Xie[2], Li Duan[1], Jianyi Xiong[1], Daping Wang[1], Shihui Zhu[6], Yujie Liang[2,7*], Jianhao Wang[3*], Jiang Xia[2*]

[1]Department of Orthopedics, Shenzhen Intelligent Orthopaedics and Biomedical Innovation Platform, Guangdong Artificial Intelligence Biomedical Innovation Platform, Shenzhen Second People's Hospital, the First Affiliated Hospital of Shenzhen University Health Science Center, Shenzhen, 518035, China
[2]Department of Chemistry, the Chinese University of Hong Kong, Shatin, Hong Kong SAR, China
[3]School of Pharmacy, Changzhou University, Changzhou, Jiangsu 213164, China
[4]Shijiazhuang Maternity and Child Health Hospital, Shijiazhuang, Hubei, 050093, China
[5]Jiangsu Trautec Medical Technology Co., Ltd, No.28 Shuanglong Road, Jintan Development Zone, Changzhou, Jiangsu, 213200, China
[6]Department of Burn Surgery, Institute of Burns, the First Affiliated Hospital, Naval Medical University, Shanghai, 200433 China
[7]Shenzhen Kangning Hospital, Shenzhen Mental Health Center, Shenzhen, Guangdong, 518020, China
[†]*These authors contributed equally to this work.*

Abstract: Artificial skins are biomaterials that can replace the lost skin or promote the regeneration of damaged skin. Skin regenerative biomaterials are highly applauded because they can exempt patients with severe burns from the painful procedure of autologous skin transplantation. Notwithstanding decades of research, biocompatible, degradable, and printable biomaterials that can effectively promote skin regeneration as a transplantation replacement in clinical use are still scarce. Here, we report one type of all-protein hydrogel material as the product of the enzymatic crosslinking reaction of gelatin and a recombinant type III collagen (rColIII) protein. Doping the rColIII protein in gelatin reduces the inflammatory response as an implant underneath the skin. The all-protein hydrogel can be bioprinted as scaffolds to support the growth and proliferation of 3T3 fibroblast cells. The hydrogel used as a wound dressing promotes wound healing in a rat model of skin damage, showing a faster and healthier recovery than the controls. The rColIII protein in the hydrogel has been shown to play a critical role in skin regeneration. Altogether, this work manifests the development of all-protein gelatin-rColIII hydrogel and demonstrates its use in wound healing. The gelatin-collagen hydrogel wound dressing thereby may become a promising treatment of severe wounds in the future.

Keywords: Gelatin; Recombinant collagen; Hydrogel; Artificial skin; Wound healing

*Correspondence to: Yujie Liang, Department of Chemistry, the Chinese University of Hong Kong, Shatin, Hong Kong SAR, China; liangyjie@126.com; Jianhao Wang, School of Pharmacy, Changzhou University, Changzhou, Jiangsu 213164, China; minuswan@163.com; Jiang Xia, Department of Chemistry, the Chinese University of Hong Kong, Shatin, Hong Kong SAR, China; jiangxia@cuhk.edu.hk.

Received: November 18, 2021; **Accepted:** December 29, 2021; **Published Online:** February 24, 2022

Citation: Huang J, Lei X, Huang Z, *et al*, 2022, Bioprinted Gelatin Recombinant Type III Collagen Hydrogel Promotes Wound Healing. *Int J Bioprint,* 8(2):517. http://doi.org/10.18063/ijb.v8i2.517

1. Introduction

The skin is the largest organ of the human body. The skin serves multiple functions, including regulation of body temperature and transmission of sensations, and also acts as a barrier to safeguard the body from the invasion of microorganisms and the damaging effects of unwanted chemical and physical stimuli. The skin is also a fragile organ; it is difficult to replace when irreversibly damaged by severe burns, trauma, or disease[1-3]. Despite

being the most common treatment for repairing severe skin defects, autologous skin transplantation has many disadvantages[4,5]. Skin from the patient's unburned area, including the dermis and epidermis, can be used to repair burned skin areas. For severe burns larger than 60% of total body surface area, multiple harvests from the donor site after healing are required. However, this procedure may increase the risk of infection and cause scarring and pigmentation changes of the donor site. In addition, patients need to endure for a long time to wait for the new skin to re-epithelize at the donor site.

At present, researchers are developing new biomaterials that can be used to replace skin for the short term or permanently; these skin substitutes are collectively called "artificial skin." To promote wound healing, the skin substitute must: (a) Adhere to the substrate, (b) has sufficient elasticity and the ability to withstand deformation, (c) allow water to evaporate at a typical rate similar to the stratum corneum, (d) has a microbial barrier, (e) promotes hemostasis and accelerates coagulation, (f) is easy to use, (g) be used immediately after injury, and (h) causes a "regeneration-like" reaction in the wound bed without causing inflammation or foreign bodies or non-self-immunologic reaction[6-8]. A successful example is given by Burke *et al*. who pioneered classical experiments of the development of dermal equivalents for biological replacement[6-8]. Briefly, starting from glutaraldehyde-cross-linked collagen, glycosaminoglycan was mixed to stimulate the synthesis of normal connective tissue matrix in the dermis without inflammation, foreign body reaction, or immunologic reaction. Years of work resulted in a product called Integra®, which contains collagen extracted from cowhide and chondroitin 6-sulfate extracted from shark cartilage to form a collagen-chondroitin-6-sulfate fiber. This product was approved the United States Food and Drug Administration for treating burn patients.

Notwithstanding the success Integra® achieved over the years, there is still much room to improve. Natural collagen purified from animal sources faces several limitations in clinical use[9-12]. For example, the quality control of collagen products from animal sources is often a challenge because of the heterogeneity of the natural collagen and the risk of pathogen contamination. The main ingredients of adult skin tissue are type I and type III collagen. In contrast, the proportion of type III collagen in fetal skin is significantly higher than that of adults[13,14]. It has been reported that the decrease of type III collagen is associated with the aging of the skin, leading to the lack of elasticity and renewability[15-18]. Supplementing the loss of type III collagen will reduce scar hyperplasia and promote skin regeneration[19]. In this regard, collagens from a natural animal source are often a mixture of different isotypes, making it difficult to delineate the role of each collagen isotype. We reason that a recombinant, pure form of type III collagen will be superior for skin regeneration[20]. This then inspired the use of recombinant technology and genetic tools to produce type III collagen *ex vivo*[21-24]. The recombinant human type III collagen (rColIII) has been used to treat full-thickness skin defects in pigs[25]. Since rColIII is highly soluble, to form a hydrogel for wound covering, we sought to use gelatin, the hydrolysate of collagen, to provide a framework of crosslinking. Gelatin has excellent biocompatibility, low immunogenicity, low toxicity, and high biodegradability. Therefore, gelatin is widely used in hemostatic wound dressings, vascular stents, drug carriers, tissue engineering stents, coating materials, etc.[26]. In this study, we synthesized gelatin-rColIII hydrogel (GRH) through enzymatic crosslinking and reported the therapeutic efficacy of the all-protein hydrogel in wound healing in a rat model of skin damage.

On the other hand, three-dimensional (3D) bioprinting is a manufacturing technology that can construct biomaterial scaffolds in a range of biomedical applications. 3D bioprinting of biomaterials can realize the precise assembly of the polymeric biomacromolecules, which provides a spatial framework for the growth of cell cultures and tissue engineering. Biomaterials amenable to 3D bioprinting should meet the following requirements[27-31]: (a) Excellent biocompatibility; (b) suitable biodegradability to allow substitution by the extracellular matrix and natural tissues; (c) suitable pore size and porosity to facilitate the exchange of oxygen, nutrients, and metabolites; (d) mechanical properties similar to the natural tissues; (e) low toxicity and immunogenicity; (f) strong plasticity; and (g) ease of processing. 3D bioprinting, in general, is achieved through several strategies including material extrusion[32,33], material jetting[34,35], and vat polymerization[36,37]. Among the three methods, extrusion-based 3D bioprinting strategies are now the most widely used for producing 3D tissue constructs. Here, we demonstrated that enzymatic crosslinking solidifies the GRH into the ink of 3D extrusion bioprinting[38]. The 3D GRH scaffold supports the growth of mouse embryonic fibroblasts.

2. Materials and methods

2.1. Materials and instruments

rColIII (purity >90%) was kindly provided by Jiangsu Chuangjian Medical Technology Co., Ltd. Dulbecco's modified Eagle's medium (DMEM) penicillin-streptomycin solution, fetal bovine serum (FBS), trypsin-EDTA, and gelatin were obtained from Sigma-Aldrich (USA). Aminoamidase was purchased from BOMEI Company (China). Cell counting kit-8 (CCK-8)

and cell live/dead staining kit were obtained from Dojindo Company (Japan). Other instruments include fluorescence microscope from Leica (Germany), scanning electron microscope (SEM) (TESCAN Company, Czech Republic), microplate reader (Thermo Company, USA), and CPD1 3D bioprinter (Shangpu Boyuan Company, China). Sprague Dawley rats were obtained from Top Biotech Biotechnology Co. Ltd. (Shenzhen, China) or Changzhou Cavens Biological Technology Co. Ltd. and allowed to acclimatize for 1 week in the laboratory.

2.2. 3D printing of the scaffolds

Gelatin and rColIII were mixed with the ratios of 1:0, 1:0.05, 1:0.1, 1:0.15, and 1:0.2 to form the hydrogel. A model was built by 3D CAD file (.stl file format). We set the wire spacing of the model at 1.5 mm and the layer height at 0.25 mm. Rectangular parallelepiped specimens with dimensions of 20 mm × 20 mm × 3 mm (length × width × height) were used. Briefly, gelatin and rColIII were sterilized by Co60 radiation. The gelatin powder was dissolved in ultrapure water (1 g gelatin and 10 ml ultrapure water are mixed to make a 10% solution, heated to 40°C, and stirred for 30 min), and rColIII was added in different proportions (0 g, 0.05 g, 0.10 g, 0.15 g, and 0.20 g). Before 3D printing, 1 ml of 10% transglutaminase aqueous solution was added for enzymatic crosslinking for 5 min. Then, 3D porous hydrogel scaffolds with a size of 20 mm × 20 mm × 3 mm were printed by a CPD1 3D printer.

2.3. Porosity measurement

Porosity is defined as the volume of the pores over the total volume of the scaffold. Ethanol occupation was used to estimate the volumes. The 3D scaffolds were lyophilized for 48 h, and the dry weight was measured. The scaffolds were then immersed in absolute ethanol and placed under a vacuum until all the pores were filled. The weight of ethanol that occupies the pores is calculated as M_p. The weight of ethanol that corresponds to the total volume of the scaffold is calculated as M_T. Porosity is then calculated as M_p/M_T. The samples were measured in triplets. The moisture content is calculated based on the weight loss of the stent after freeze-drying. The swelling curve of the material was calculated by measuring the water absorption of the freeze-dried scaffold at different time points.

2.4. SEM analysis

Scaffolds were sliced into samples of 4 mm × 4 mm × 3 mm sizes, fixed in 2.5% glutaraldehyde solution, dehydrated gradually from 50% up to 100% ethanol, displaced with isopropyl acetate, and freeze-dried for 48 h before being processed for SEM imaging.

2.5. Proliferation assay

NIH-3T3 cells were cultured in DMEM containing 10% FBS and 1% penicillin/streptomycin at 37°C under the ambience of 5% CO_2. Cells were seeded on the scaffold at a density of 1.0×10^5 per scaffold. In the control group, cells were grown on 48-well plates. Then, the CCK-8 kit was used to measure the number of cells at different time points.

2.6. Subcutaneous implantation assay

All the animal experiments have been approved by the ethics committee of Shenzhen Top Biotech Co. Ltd. (no. TOP-IACUC-2020-09-0007). Hydrogel samples were implanted subcutaneously in rats to evaluate biocompatibility *in vivo*. After the rats were anesthetized with 1.5% isoflurane, the dorsal region was disinfected, and an incision of about 2 cm was made. A sterile hydrogel cube of 1 cm in length and width and 3 mm in thickness was implanted. The incision was sutured with 4-0 sutures. After implantation for 4 weeks, the rats were anesthetized and killed. The back hydrogel and surrounding tissues were taken out together and fixed with 4% paraformaldehyde. After dehydration, they were embedded in paraffin and cut into pathological sections. The sections were stained with hematoxylin and eosin (HE), and immunohistochemical staining was applied to quantify the inflammatory factors such as CD68, interleukin (IL)-10, and tumor necrosis factor-alpha (TNF-α). Immunohistochemical staining was performed as previously reported[39]. The primary antibodies used in this experiment were anti-collagen I, anti-collagen III, anti-IL-10, anti-TNF-α, and anti-CD68 antibodies (Abcam, Cambridge, MA, UK).

2.7. Cell live-dead staining

NIH-3T3 cells were inoculated into the hydrogel for 1, 4, and 7 days in separate experiments. After inoculation, cells were then stained with calcein AM (2 μM) and propidium iodide (3 μM) for 20 min at 37°C before imaging under a fluorescence microscope.

2.8. Animal wound treatment

Briefly, male adult Sprague Dawley rats (180–220 g) were kept in polypropylene cages with free access to water and food. Animals were divided into four groups, and each group contained six animals: A, PBS control; B, GRH_0 group; C, GRH_{10} group; and D, GRH_{20} group. All rats were anesthetized with sodium phenobarbitone before surgery. Then, the dorsal surface of rats was surgically manipulated to remove one full-thickness skin wound (diameter = 2 cm) under aseptic conditions. A 2 ml hydrogel materials were then applied to the surface of the wounds and bandage, and the dressing was changed

every 2 days. Photographs of skin wound healing were taken on days 1, 3, 5, 7, 9, 11, and 13 to observe the skin recovery. The rats were sacrificed on days 1, 7, and 13 after the operation. The wound bed and the surrounding healthy skin were collected. Full-thickness skin samples, wound edges, and epithelialized wounds were prepared for tissue sections.

2.9. Histological evaluation of wound regeneration

For histological staining analysis, the wound skin tissues were taken out on days 1, 7, and 13. The excised skin samples were first fixed with 10% formalin, then dehydrated by ethanol gradient incubation, embedded in paraffin, and cut into sections with a thickness of 8 μm. As a part of the histopathological evaluation, tissue sections were stained with HE, Masson's trichrome stain, and Sirius red stain to determine collagen formation status.

3. Results and discussion

3.1. GRH scaffolds

Doping rColIII protein to gelatin at different ratios, followed by crosslinking by transglutaminase, gives a series of GRH materials amenable to 3D printing. We thereby constructed GRH scaffolds: GRH_0, GRH_5, GRH_{10}, GRH_{15}, and GRH_{20} with 0%, 5%, 10%, 15%, and 20% of rColIII in gelatin, respectively. These GRH materials were then printed into scaffolds with sizes of 20 mm × 20 mm × 3 mm and grids of about 1 mm (**Figure 1A**). SEM analysis showed that these materials had a rough surface amenable for cell adhesion (**Figure 1B**). All five GRHs were highly porous and rich in water (**Figure 2A** and **B**). The lyophilized GRHs reached the maximal water absorption after 4 h during the hydration process. An increasing amount of rColIII corresponded to the decreasing level of swelling in the solution (**Figure 2C**). The Fourier transform infrared (FTIR) spectra of the hydrogels show several characteristic bands of protein-based materials (**Figure S1**). The vibration of amide A bands at around 3290 cm^{-1} and 3300 cm^{-1} indicates hydrogen bonds. The amide I bands at 1638 cm^{-1} and 1633 cm^{-1} correspond to the vibration of the C=O bond, suggesting the existence of the secondary structure of the polypeptide in the protein material. The amide II bands appear at 1550 cm^{-1} and 1541 cm^{-1}, indicating the stretching vibration of the C-N bond and the bending vibration of the N-H bond, respectively. Amide III bands appear at 1239 cm^{-1} and 1238 cm^{-1}, indicating that the triple helix structure of gelatin molecules is still maintained in the hydrogel. The peak at 1450 cm^{-1} corresponds to the cis structure of the peptide bond. The infrared spectrum of the hydrogel has a strong serine side group C-O stretching vibration absorption peak near 1024 cm^{-1}, which is a characteristic peak of type III collagen.

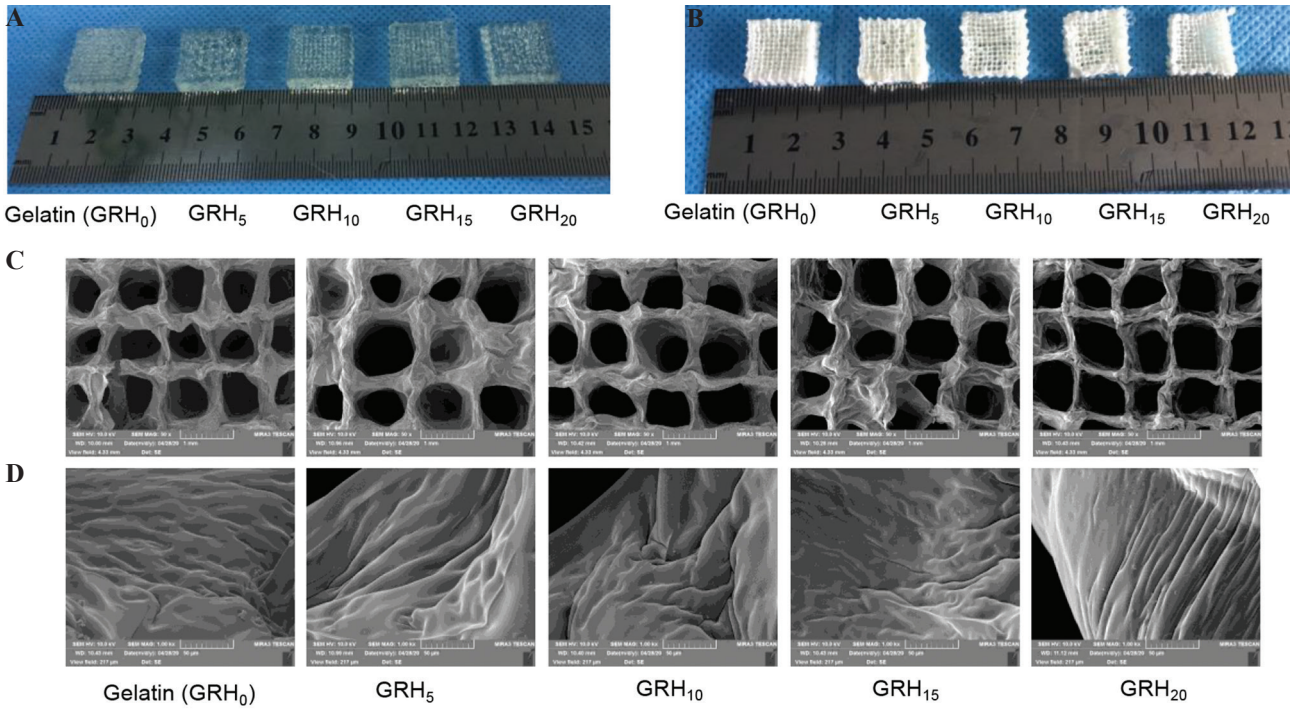

Figure 1. Morphology of gelatin rColIII hydrogel (GRH) scaffolds. Images of the GRH scaffolds in wet (A) and lyophilized form (B). Scanning electron microscope images of the GRH scaffolds in 50× (C) and 1000× (D).

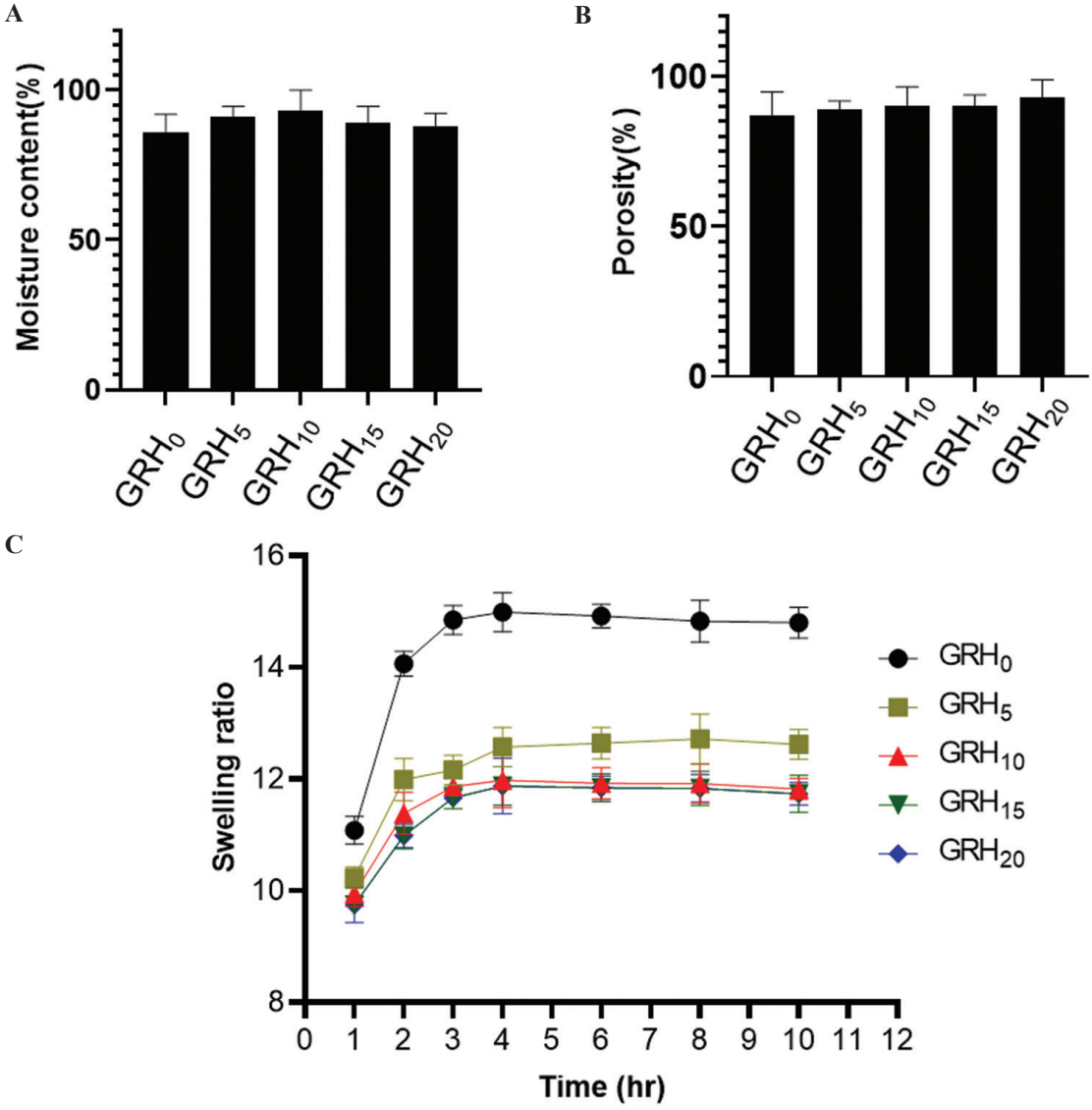

Figure 2. Physical properties of gelatin rColIII hydrogel. (A) Moisture content. (B) Porosity. (C) Swelling kinetics.

3.2. Biocompatibility of the GRHs

To study the material's biocompatibility *in vivo*, the stent was implanted subcutaneously in rats for 28 days. After the 28-day incubation, we explored the inflammatory response of the surrounding tissue by immunohistochemical analyses of IL-10, TNF-α, and CD68 (**Figure 3**). In the GRH_0 group, residual gelatin remained after the 28-day incubation, and the implant material was completely degraded in the other groups. HE staining of the GRH_{20} group showed that the number of monocytes and macrophages was reduced. GRH_{20} group also showed lower expression of the inflammatory factors such as IL-10, TNF-α, and CD68 (indicated by level of staining). We also observed that the GRH_{20} hydrogel was significantly degraded as compared to other samples (**Figure S2**). Therefore, the recombinant type III collagen (rColIII) protein may increase the absorption of GRH implant and alleviate the inflammatory response of the gelatin hydrogel.

3.3. Cell adhesion and proliferation on GRH scaffolds in vitro

We next explored whether the GRH scaffolds can support the adhesion and proliferation of NIH 3T3 cells, a cell line of mouse embryonic fibroblasts. All four GRH scaffolds support cell proliferation based on CCK8 analysis (**Figure S3**). We incubated the cells on the GRH scaffolds for 1, 4, and 7 days and stained them with calcein AM for the live cells (green fluorescence) and propidium iodide for the dead cells (red fluorescence) (**Figure 4**). Most cells grew on the scaffolds instead of in the cavities or on the bottom of

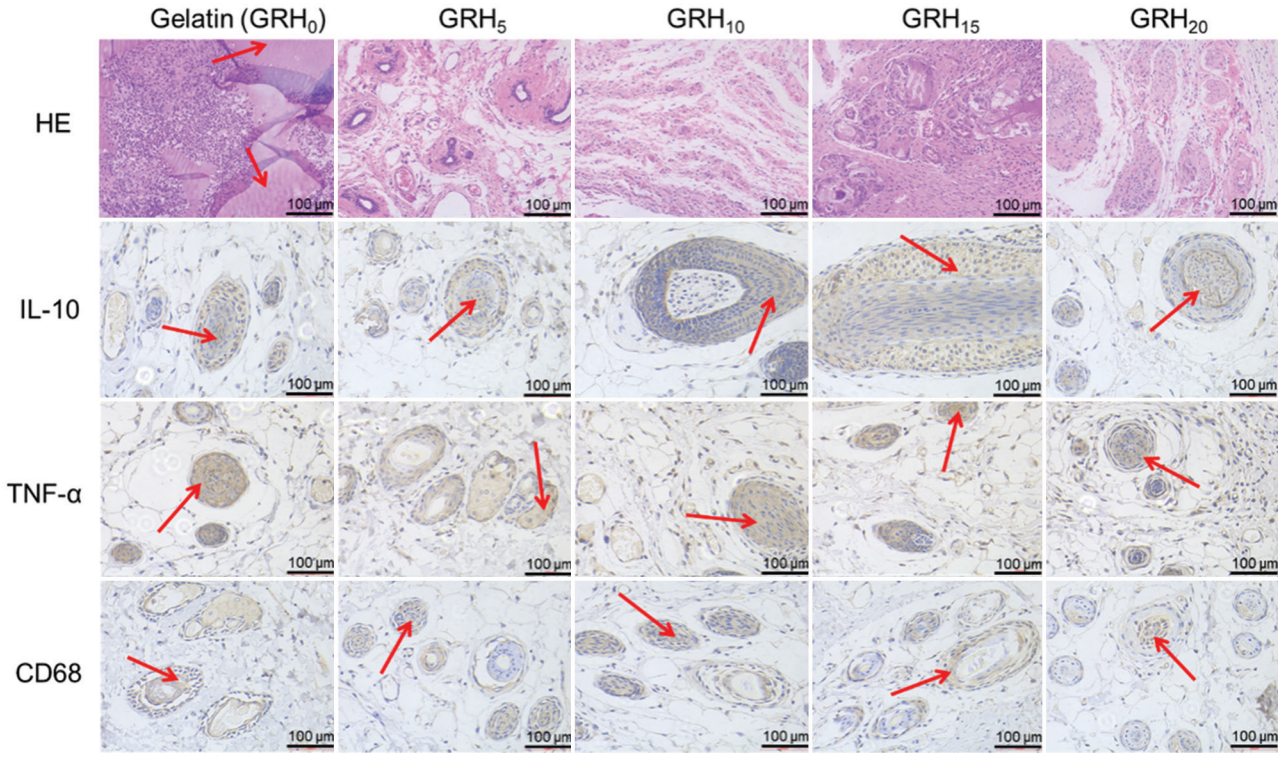

Figure 3. Immunohistochemical staining of tissues surrounding different implants. Arrows in the HE staining show the residual hydrogel material. Arrows in other panels show areas of interest where high staining signals are detected. Scale bar: 100 μm.

the cell culture dish. All five GRH scaffolds support the adhesion, proliferation, and migration of NIH 3T3 cells.

3.4. Promotion of wound healing in a rat model

Finally, we examined whether the GRH hydrogels can be used as dressing materials to promote wound healing in a rat model of skin damage. Briefly, full-thickness skin wounds (diameter = 2 cm) were created on the dorsal surface of rats, and hydrogel materials were then applied to the surface of the wounds. After a designated duration of incubation, the skin samples were removed and analyzed by various methods. First, the wound sizes in different groups were recorded. We observed a trend that the higher percentage of the type III collagen component corresponds with increasing wound healing rate, and in the GRH_{20} group, the wound healed almost completely after 13 days, which was significantly faster than all other groups (**Figure 5**).

The quality of the wound healing was then analyzed by various staining of the tissue samples at the wound areas. Rats were sacrificed on day 7 or 13, and the wound areas were dissected and stained by HE staining. In the control group in which rats were treated with PBS, the formation of scab and necrotic tissue agglomeration was observed in the absence of epidermis, hair follicles, or blood vessels on day 7. Only a small number of new collagen fibers were formed with disordered distributions on day 13 in this group (**Figure 6**). This shows that although adult rats can self-regenerate wounded skins to a certain degree, the regeneration process took longer than 2 weeks. All three GRH treatment groups showed promising healing results, and the higher concentration of rColIII corresponded to more complete skin regeneration. For example, on day 13, the wounds in PBS control and GRH_0 groups showed disorganized tissue structures. On the contrary, in both GRH_{10} and GRH_{20} groups, dense tissue structures with the ordered arrangement and obvious cuticle were seen (**Figure 6**), which is a sign of the emergence of healthy skin tissues.

The same tissue was also stained by Masson's trichrome; the blue marks represent collagen fibers, and the red marks represent muscle fibers. On day 7, scar formation or tissue hyperplasia, indicated by the predominant red color, occurred at the wound area in the PBS control and GRH_0 groups. In contrast, significantly higher level of collagen fibers was observed in the GRH_{10} and GRH_{20} groups (**Figure 7**). Consistently, this demonstrates healthy healing due to rColIII in the wound dressing material. The same trend was also observed in the staining images of the day 13 samples (**Figure 7**). Quantification of the staining signals highlighted the differences (**Figure 7B**).

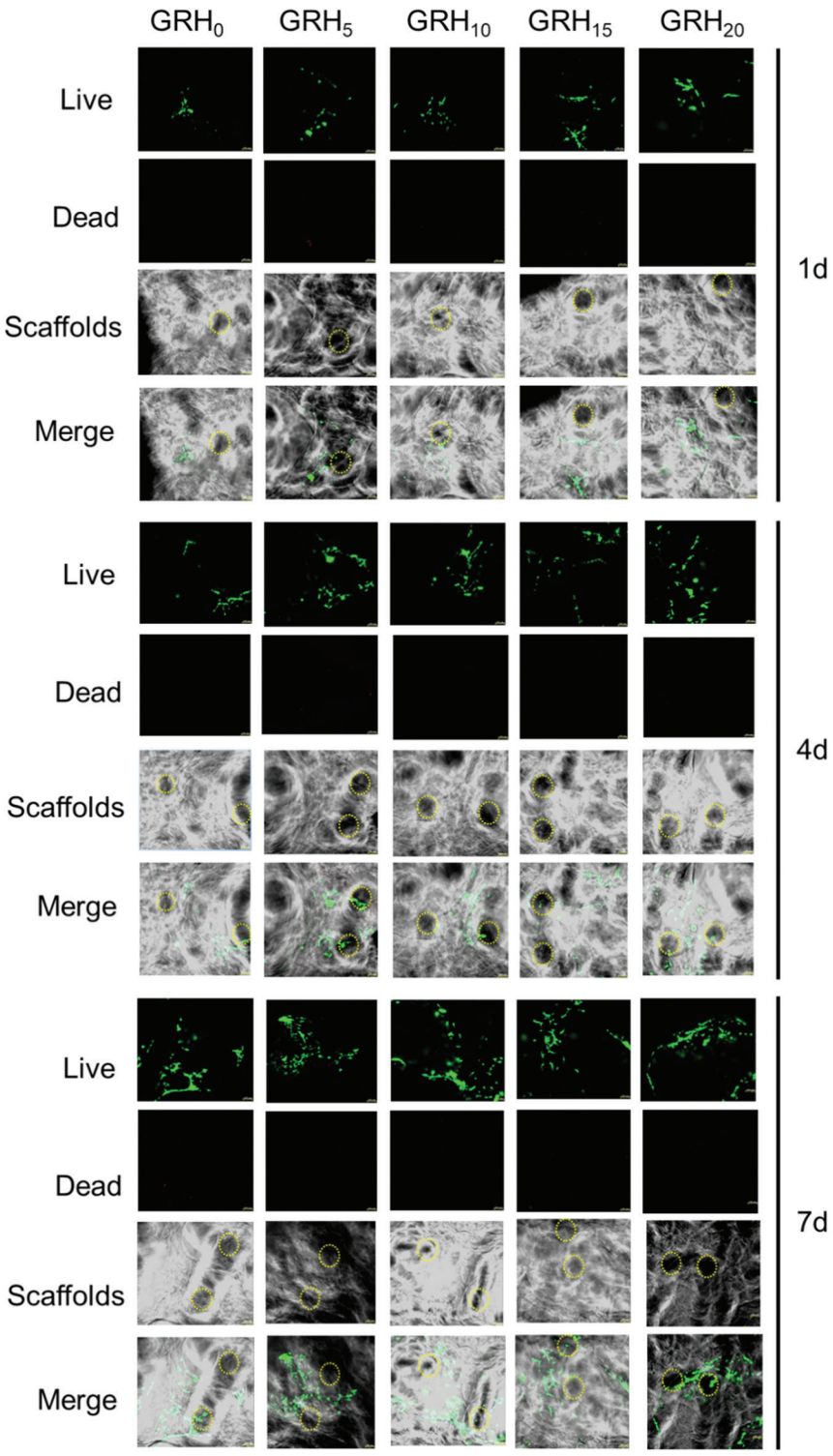

Figure 4. Cell proliferation on the scaffolds based on the live/dead staining. Images of 1d, 4d, and 7d are representative images of cell cultures incubated on the scaffold for 1 day, 4 days, and 7 days, representatively. The cavities of the scaffolds are marked. Scale bar: 100 μm.

Finally, after Sirius red staining of the tissue section can be seen as orange for type I collagen and type III collagen was stained orange and bright green for type III collagen, respectively, confirming collagen deposition at the wound. During the skin healing process, the collagen content of all groups increased. However, the PBS control group and GRH_0 group were dominated by the formation of type I collagen. On

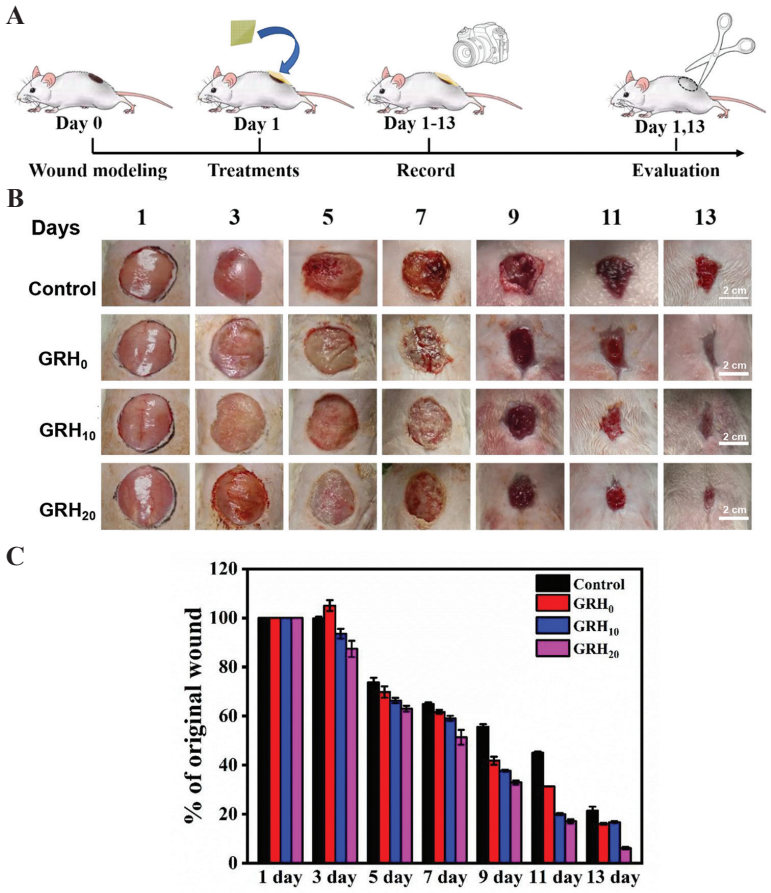

Figure 5. Gelatin rColIII hydrogel coating promotes wound closure. (A) Schematic illustration of the experimental procedure. (B) Representative photographs of wounds in four groups during the 13-day treatment. Scale bar: 2 cm. (C) Quantification of the relative sizes of the wounds (% of the original dimensions of the wounds). Data were expressed as standard deviations (n=6).

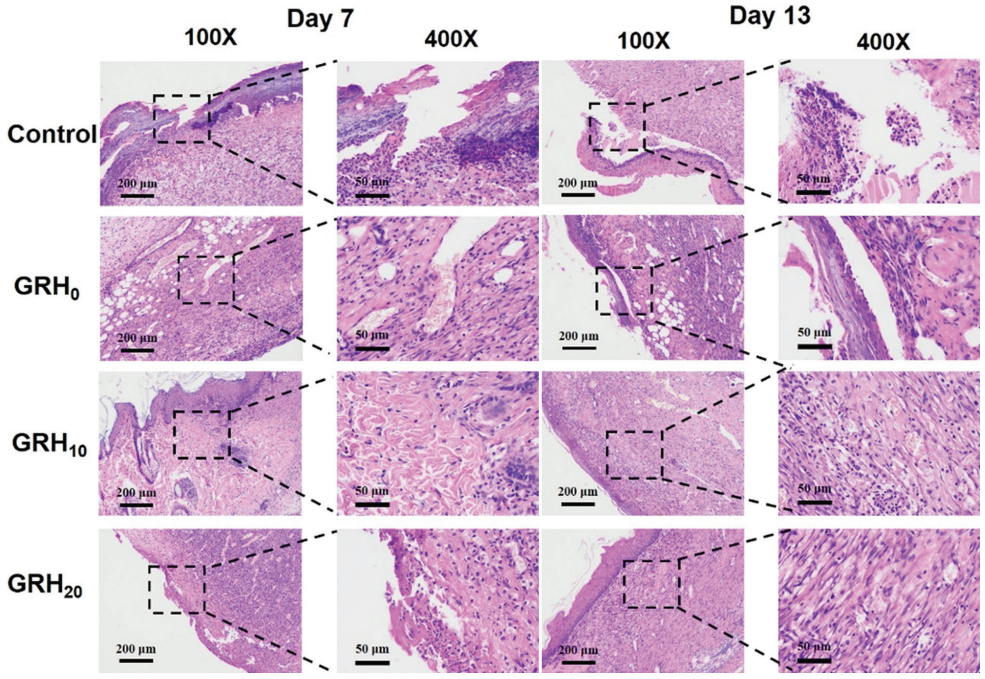

Figure 6. Representative HE staining images of the skin tissues of rat wounds in four different groups.

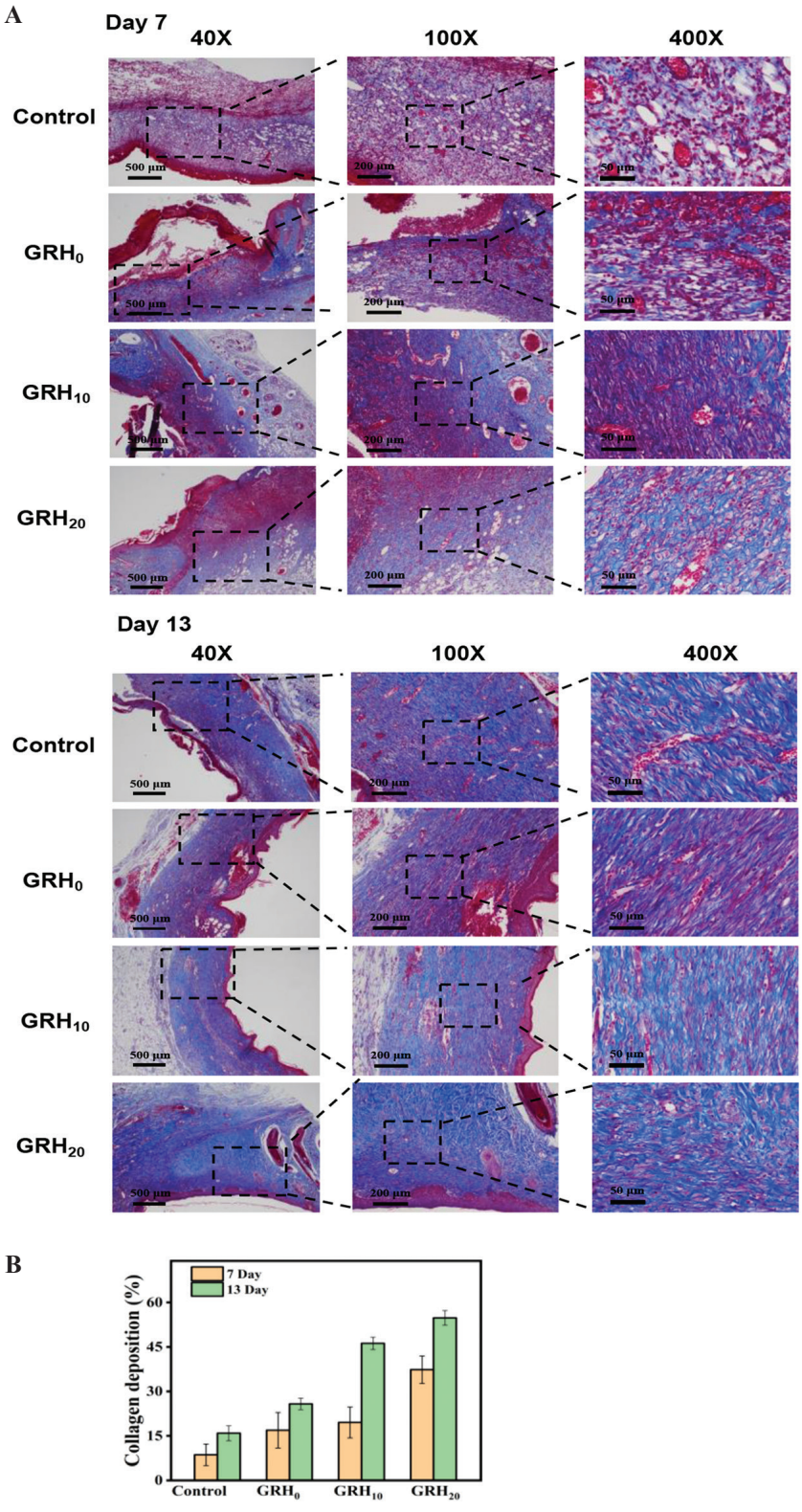

Figure 7. Masson's trichrome staining images and the corresponding quantification of the collagen deposition in four different groups.

the contrary, a significantly higher amount of type III collagen was observed in the GRH_{20} group (**Figure 8**), with less wound scar contracture and sclerosis. These findings altogether indicate that more advanced and

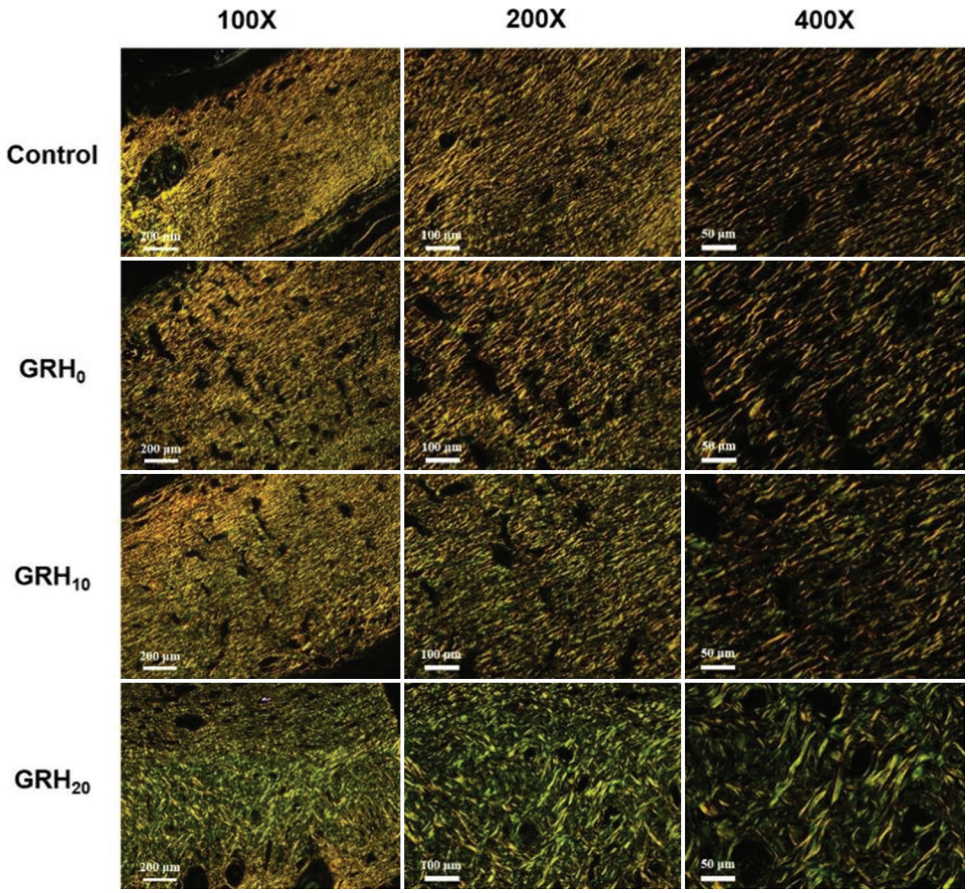

Figure 8. Sirius red staining images of the skin tissues of the rat wounds in four different groups on day 13. Scale bar: 200 μm.

high-quality wound healing was achieved in the GRH_{20} group compared to other groups.

4. Conclusion

Artificial skins as the wound covering materials that promote the regeneration of damaged skins can alleviate the pain of patients with severe skin damage. Yet, an optimal composition of the covering materials that lead to a high-quality, rapid wound healing has still not been found. In this study, we showed that gelatin alone is insufficient to provide an environment for damaged skin tissues to heal rapidly. The addition of rColIII can significantly accelerate the speed of wound healing and improve the quality of repair, as evidenced by a substantially smaller wound area, denser tissue structures with an ordered arrangement and obvious cuticle, a significantly higher amount of collagen fibers instead of muscle fibers, and a higher level of nascent collagens, especially the type III collagen. Taken together, we present an all-protein hydrogel material composed of gelatin and rColIII that can be used for wound healing in patients with severe skin damage.

Acknowledgments

We acknowledge funding supports by Jiangsu Key Research and Development Plan (Society Development, No. BE2018639), the Qinglan Project of Jiangsu Province, Shenzhen Science and Technology Projects (GJHZ20190820115203714, JSGG20191129094218565), Sanming Project of Medicine in Shenzhen (SZSM201612079), Shenzhen Fund for Guangdong Provincial High Level Clinical Key Specialties (No. SZGSP013, SZGSP007), and Shenzhen Key Medical Discipline Construction Fund (SZXK042 and SZXK049). This work was partially funded by the University Grants Committee of Hong Kong (GRF Grants N_CUHK422/18) and CUHK RSFS grant.

Conflicts of interest

No author has financial or other contractual disagreements that might cause conflicts of interest.

Author contributions

J.H., H.L., and J. Xia designed the research. J.H., X.L., Z.H., Z.R., and Y.X. performed the research. L.D., J.

Xiong, D.W., and Y.L. analyzed the data. X.L., Y.L., J.W., and J. Xia wrote the paper.

References

1. Martin P, 1997, Wound Healing--Aiming for Perfect Skin Regeneration. *Science*, 276:75–81. https://doi.org/10.1126/science.276.5309.75
2. Reinke JM, Sorg H, 2012, Wound Repair and Regeneration. *Eur Surg Res*, 49:35–43. https://doi.org/10.1159/000339613
3. Heng M, 2011, Wound Healing in Adult Skin: Aiming for Perfect Regeneration. *Int J Dermatol*, 50:1058–66. https://doi.org/10.1111/j.1365-4632.2011.04940.x
4. Fleischmann T, Nicholls F, Lipiski M, *et al*., 2019, Transplantation of Autologous Dermo-epidermal Skin Substitutes in a Pig Model. *Methods Mol Biol*, 1993:251–9. https://doi.org/10.1007/978-1-4939-9473-1_20
5. Herskovitz I, Hughes OB, Macquhae F, *et al*., 2016, Epidermal Skin Grafting. *Int Wound J*, 3:52–6. https://doi.org/10.1111/iwj.12631
6. Schulz JT 3rd, Tompkins RG, Burke JF, *et al*., 2020, Artificial Skin. *Annu Rev Med*, 51:231–44. https://doi.org/10.1146/annurev.med.51.1.231
7. Vig K, Chaudhari A, Tripathi S, *et al*., 2017, Advances in Skin Regeneration Using Tissue Engineering. *Int J Mol Sci*, 18:789. https://doi.org/10.3390/ijms18040789
8. Bhardwaj N, Chouhan D, Mandal BB, (2017) Tissue engineered skin and wound Healing: current strategies and future directions. *Curr Pharm Des*, 23:3455–82. https://doi.org/10.2174/1381612823666170526094606
9. Sorushanova A, Delgado LM, Wu Z, *et al*., 2019, The Collagen Suprafamily: From Biosynthesis to Advanced Biomaterial Development. *Adv Mater*, 31:e1801651. https://doi.org/10.1002/adma.201801651
10. Rodríguez MI, Barroso LG, Sánchez ML, 2018, Collagen: A Review on its Sources and Potential Cosmetic Applications. *J Cosmet Dermatol*, 17:20–6. https://doi.org/10.1111/jocd.12450
11. Davison-Kotler E, Marshall WS, García-Gareta E, 2019, Sources of Collagen for Biomaterials in Skin Wound Healing. *Bioengineering*, 6:56. https://doi.org/10.3390/bioengineering6030056
12. Browne S, Zeugolis DI, Pandit A, 2013, Collagen: Finding a Solution for the Source. *Tissue Eng Part A*, 19:1491–4. https://doi.org/10.1089/ten.TEA.2012.0721
13. Liu X, Hong WU, Byrne M, *et al*., 1997, Type III Collagen is Crucial for Collagen I Fibrillogenesis and for Normal Cardiovascular Development. *Proc Natl Acad Sci U S A*, 94:1852–6.
14. Clore JN, Cohen IK, Diegelmann RF, 1979, Quantitation of Collagen Types I and III during Wound Healing in Rat Skin. *Proc Soc Exp Biol Med*, 161:337–40. https://doi.org/10.3181/00379727-161-40548
15. Gay S, Vijanto J, Raekallio J, *et al*., 1978, Collagen Types in Early Phases of Wound Healing in Children. *Acta Chir Scand*, 144:205–11.
16. Mays PK, Bishop JE, Laurent GJ, 1988, Age-related Changes in the Proportion of Types I and III Collagen. *Mech Ageing Dev*, 45:203–12. https://doi.org/10.1016/0047-6374(88)90002-4
17. Podolsky MJ, Yang CD, Lizama C, *et al*., 2020, Age-dependent Regulation of Cell-mediated Collagen Turnover. *JCI Insight*, 5:e137519. https://doi.org/10.1172/jci.insight.137519
18. Wang C, Rong YH, Ning FG, *et al*., The Content and Ratio of Type I and III Collagen in Skin Differ with Age and Injury. *Afr J Biotechnol*, 10:2524–9.
19. Leung A, Crombleholme TM, Keswani SG, 2012, Fetal Wound Healing: Implications for Minimal Scar Formation. *Curr Opin Pediatr*, 24:371–8. https://doi.org/10.1097/MOP.0b013e3283535790
20. Chattopadhyay S, Raines RT, 2014, Review Collagen-based Biomaterials for Wound Healing. *Biopolymers*, 101:821–33. https://doi.org/10.1002/bip.22486
21. Báez J, Olsen D, Polarek JW, 2005, Recombinant Microbial Systems for the Production of Human Collagen and Gelatin. *Appl Microbiol Biotechnol*, 69:245–52. https://doi.org/10.1007/s00253-005-0180-x
22. Myllyharju J, Nokelainen M, Vuorela A, *et al*., 2000, Expression of Recombinant Human Type I-III Collagens in the Yeast Pichia pastoris. *Biochem Soc T*, 28:353–7.
23. Olsen D, Yang C, Bodo M, *et al*., 2003, Recombinant Collagen and Gelatin for Drug Delivery. *Adv Drug Deliv Rev*, 55:1547–67. https://doi.org/10.1016/j.addr.2003.08.008
24. Shoseyov O, Posen Y, Grynspan F, 2014, Human Collagen Produced in Plants: More than Just Another Molecule. *Bioengineered*, 5:49–52. https://doi.org/10.4161/bioe.26002
25. Liu T, Zheng X, Li H, *et al*., 2019, Effect of Recombinant Human Type-III Collagen Hydrogels on Wound Healing of Pig Full-thickness Skin Defects. *Chin J Injury Repair Wound Healing*, 14:97–102.
26. Echave MC, Burgo L, Pedraz JL, *et al*., 2017, Gelatin as Biomaterial for Tissue Engineering. *Curr Pharm Des*,

23:3567–84.
https://doi.org/10.2174/0929867324666170511123101

27. Skardal A, Atala A, 2015, Biomaterials for Integration with 3-D Bioprinting. *Ann Biomed Eng*, 42:730–46.
https://doi.org/10.1007/s10439-014-1207-1
28. Jungst T, Smolan W, Schacht K, *et al*., 2016, Strategies and Molecular Design Criteria for 3D Printable Hydrogels. *Chem Rev*, 116:1496–539.
https://doi.org/10.1021/acs.chemrev.5b00303
29. Blaeser A, Campos DF, Puster U, *et al*., 2016, Controlling Shear Stress in 3D Bioprinting is a Key Factor to Balance Printing Resolution and Stem Cell Integrity. *Adv Healthc Mater*, 5:326–33.
https://doi.org/10.1002/adhm.201500677
30. Billiet T, Vandenhaute M, Schelfhout J, *et al*., 2012, A Review of Trends and Limitations in Hydrogel-rapid Prototyping for Tissue Engineering. *Biomaterials*, 33:6020–41.
https://doi.org/10.1016/j.biomaterials.2012.04.050
31. Highley CB, Rodell CB, Burdick JA, 2015, Direct 3D Printing of Shear-Thinning Hydrogels into Self-Healing Hydrogels. *Adv Mater*, 27:5075–9.
https://doi.org/10.1002/adma.201501234
32. Zhang YS, Haghiashtiani G, Hübscher T, *et al*., 3D Extrusion Bioprinting. *Nat Rev Methods Primers*, 1:75.
33. Ramesh S, Harrysson OL, Rao PK, *et al*., 2021, Extrusion Bioprinting: Recent Progress, Challenges, and Future Opportunities. *Bioprinting*, 21:e00116.
34. Ng WL, Huang X, Shkolnikov V, *et al*., 2022, Controlling Droplet Impact Velocity and Droplet Volume: Key Factors to Achieving High Cell Viability in Sub-Nanoliter Droplet-based Bioprinting. *Int J Bioprinting*, 8:424.
35. Li X, Liu B, Pei B, *et al*., 2020, Inkjet Bioprinting of Biomaterials. *Chem Rev*, 120:10793–833.
36. Ng WL, Lee JM, Zhou M, *et al*., 2020, Vat Polymerization-based Bioprinting-process, Materials, Applications and Regulatory Challenges. *Biofabrication*, 12:022001.
37. Li W, Mille LS, Robledo JA, *et al*., 2020, Recent Advances in Formulating and Processing Biomaterial Inks for Vat Polymerization-Based 3D Printing. *Adv Healthc Mater*, 9:e2000156.
https://doi.org/10.1002/adhm.202000156
38. Huang J, Huang Z, Liang Y, *et al*., 2012. 3D Printed Gelatin/Hydroxyapatite Scaffolds for Stem Cell Chondrogenic Differentiation and Articular Cartilage Repair. *Biomater Sci*, 9:2620–30.
39. Akutsu T, Ikegaya H, Watanabe K, *et al*., 2019, Immunohistochemical Staining of Skin-expressed Proteins to Identify Exfoliated Epidermal Cells for Forensic Purposes. *Forensic Sci Int*, 303:109940.
https://doi.org/10.1016/j.forsciint.2019.109940

Publisher's note